Structural and Geomicrobiological Characteristics of a Microbial Community From a Cold Sulfide Spring

Susanne Douglas*[1] and Dean D. Douglas[2]

[1]Astrobiology Research Element, NASA Jet Propulsion Laboratory,
4800 Oak Grove Dr., Pasadena, CA 91109
[2]Department of Microbiology,
University of Guelph, Guelph, Ont. N1G 2W1, Canada

Key Words: sulfur spring, green sulfur bacteria, purple sulfur bacteria, cyanobacteria

*To whom correspondence should be addressed. Email: Susanne.Douglas@jpl.nasa.gov
Phone: (818)354-6322; Fax: (818)393-4445

ABSTRACT

The Ancaster sulfur spring is a cold (9°C) sulfur spring located near Ancaster, Ontario, Canada which hosts an abundant and diverse micobial mat community.We have conducted an extensive microscopical study of this spring using a number of techniques: phase light, confocal scanning laser microscopy, conventional scanning electron microscopy using both chemical/critical point drying and cryofixation preparative techniques, environmental scanning electron microscopy, and transmission electron microscopy. With the latter two techniques we also used energy dispersive xray spectroscopy for elemental analysis to complement wet geochemical data collected on bulk spring water and mat pore water. This approach allowed us to gain an appreciation of the characteristics of this microbial community on a variety of length scales and allowed us to develop a good understanding of the types of microorganisms present in this community, inferring some of the relationships among its members. In the spring, different mat types existed, based on differing colours and textures, due to the predominance of specific microbial groups. Segregation of these types and examination by microscopy showed that all the major groups of sulfide-oxidising bacteria, purple bacteria, green bacteria, cyanobacteria, and colourless sulfur oxidising bacteria were represented. In some cases there seemed to be types present that have not previously been described in the literature; we hope to learn more about these as we pursue phylogenetic analysis of the Ancaster sulfur spring community. In the present study, we describe the members of these groups, in terms of their structural characteristics, and how their activity may relate to some of the minerals found in association with them. In addition, we wish to convey the utility of a thorough microscopical approach in microbial ecological studies.

INTRODUCTION

There are many types of microorganisms which can oxidise H_2S in order to derive energy for metabolism. The details of the physiological pathways by which they do this are numerous and are only known in detail for a few groups of organisms. However, use of H_2S can be divided into two main metabolic modes, photosynthetic and non-photosynthetic. Bacteria which use H_2S as an electron donor for photosynthesis are pigmented and therefore tend to form coloured masses when present in large numbers. Because of the tendency for H_2S to abiotically oxidise in the presence of oxygen, these organisms occur in the anoxic zones of environments which are rich in dissolved H_2S.

There are three main groups of phototrophic H_2S oxidisers, two of these, the green (sulfur) bacteria and the purple (sulfur) bacteria, are very similar in their overall physiology and ecology. Members of each of these groups can use H_2S as an electron donor for photosynthesis while being either autotrophic or heterotrophic with respect to their carbon source (Pfennig and Trüper 1989). Depending on the particular species, H_2S may be completely oxidised to sulfate (the purple and green "nonsulfur" bacteria) or may be partially oxidised to elemental S which is ususally deposited as a hydrated spherical colloid (Steudel, 1989) intracellularly (purple "sulfur" bacteria) or extracellularly (green "sulfur" bacteria). When H_2S becomes limiting, the colloidal S can be further oxidised to sulfate. The two groups differ in their tolerance for H_2S with the green sulfur bacteria being able to withstand higher levels of H_2S than the purple sulfur bacteria (Pfennig and Trüper 1989). Consequently, in still water environments, these two bacterial groups usually coexist in specific layers with the purple sulfur bacteria closer to the water surface than the green sulfur bacteria but still in the anoxic region of the water column (Canfield and Des Marais 1993). When these are present in biofilms or mats they appear as coloured zones with the pink (purple sulfur bacteria) layer overlying

the brown-green (green sulfur bacteria) layer (D'Amelio et al. 1989). This spatial relationship is also reflected in the relative oxygen tolerance of the two types. Green sulfur bacteria are strict anaerobes, rapidly killed by oxygen, while purple sulfur bacteria show varying tolerance for oxygen with some types, particularly those from saline alkaline lakes, being able to grow heterotrophically in the dark as aerobes but being intolerant of simultaneous exposure to light and oxygen (Pfennig and Trüper 1989).

Cyanobacteria are generally oxygenic phototrophs but some types have been proven capable of using H_2S as an electron donor under anoxic conditions where this compound is available (Cohen et al. 1975; Oren and Padan 1978). When engaged in anoxygenic photosynthesis, colloidal (elemental) sulfur appears to be the sole metabolic end product and is deposited extracellularly, often as small spheres attached to the cyanobacterial filament. Cyanobacteriacan perform anoxygenic photosynthesis over a wide range of H_2S levels (from 0.1 mM to 9.5 mM at neutral pH; Cohen et al. 1986). In these cyanobacteria sulfide is more toxic to oxygenic (inhibited by 0.1mM H_2S in *Oscillatoria limnetica*) than to anoxygenic photosynthesis (partially inhibited by 4 mM H_2S) so that in high sulfide environments, little contribution from oxygenic photosynthesis can be expected (Garlick et al., 1977). The greater sulfide tolerance of anoxygenic photosynthesis is a selective advantage in sulfide rich environments. While some cyanobacteria cannot grow continuously under strictly anoxic conditions, using this strategy as a temporary survival mechanism, others can maintain continuous growth under these conditions (Oren et al., 1977). This may explain the lack of cyanobacterial diversity in the Ancaster sulfur spring.

The nonphotosynthetic (colourless) sulfur oxidising bacteria, occur in two main forms, unicellular (primarily of the genera *Thiobacillus* and *Thiomicrospira*), and filamentous (the genera

Beggiatoa, *Thioploca*, and *Thiothrix*; Jørgensen, 1982; Nelson, 1989). Like the phototrophs, these bacteria may also use either organic or inorganic carbon sources and gain energy from H_2S oxidation with concommitant deposition of S^0 as intracellular (filamentous types) or extracellular (unicellular) colloidal spheres. The best-studied examples of these types of bacteria are from marine systems, especially at deep sea hydrothermal vents, where their chemoautotrophic metabolism makes them one of the only primary producers in that particular ecosystem (Jannasch 1995). Mass occurences of these organisms have also been found in freshwater habitats but they are less common here due to less readily available sources of sulfide which is generated in sea water from bacterial reduction of the abundant sulfate present.

Colourless sulfur oxidising bacteria are dependent for their metabolism upon a chemical gradient comprised of a juxtaposition between O_2 and H_2S at concentrations conducive to the existence of both as separate chemical species (Nelson and Jannasch, 1983). Thus, massive occurences of colourless sulfur oxidising bacteria mark the existence of a specific O_2/H_2S gradient. Such gradients can lead to the formation of bacterial "plates" only millimetres thick in sediments where the source of sulfide is often the activity of sulfate reducing bacteria deeper in the sediment (Larkin and Strohl 1983).

In this study we describe the microbial community and its associated inorganic constituents in the Ancaster sulfur spring, a cold, freshwater, sulfide rich spring. We also compare what can be learned from various microscopical techniques, introducing the characteristics of the mat community as revealed by environmental scanning electron microscopy (ESEM), a technique by which fully hydrated specimens can be viewed using an electron beam combined with elemental analysis by energy dispersive xray spectroscopy (EDS).

MATERIALS AND METHODS

Collection of mat and water samples. Mat samples were collected as adherent growth through removal of leaves and sticks from the spring to small 250-mL sterile wide mouth Mason jars with one mat type (based on colour and sample site) per jar. Enough spring water to fill the jar was added and the lid screwed tightly on while the jar was still under water (for the source mats). For the downstream mats, a small (ca. 2-cm) head space was maintained.

Water samples for analysis by ICP were collected as follows: For the bulk spring water samples, water was collected using 60-mL syringes and injected into N_2-purged 250-mL serum bottles. Samples were collected in triplicate and one of each set had sterile Zn acetate added to it to a final concentration of 5 mM to preserve the sulfide present. Mat pore water was collected by removing mat-covered leaves from the spring, shaking off excess water, and scraping the mat material off the leaves with sterile scalpels into the barrels of 60-mL syringes until they were full of loosely packed material. the plunger was then attached and the mats were squeezed to release pore water into 100-mL stoppered N_2-purged serum vials using a syringe-mounted sterile 0.22 μm filter. The filters had to be changed frequently as they clogged. This, again was done in triplicate, with Zn acetate added to one set.

Light microscopy. In the laboratory, mat samples were removed from the jars using long, sterile forceps and teased apart on microscope slides, using ultrapure water (i.e., water deionised to 18 $M\Omega cm^{-1}$) as the mounting matrix. The samples were viewed using a Nikon Eclipse E600 microscope optimised for phase imaging. Images were collected digitally using a Spot camera (Diagnostic

instruments, Inc.).

Scanning Electron Microscopy (SEM). To prepare mat samples for SEM, the follwing procedure was followed: Mat pieces were removed from sample jars using long, sterile forceps and placed in 7-mL borosilicate vials. The mat pieces were immersed in a solution of spring water and glutaraldehyde to a final glutaraldehyde concentration of 3% (v/v) and left overnight at 4°C. The following day, the samples were washed in three changes of ultrapure water and then immersed in 2% osmic acid (aqueous) for 2 hours at room temperature. They were then washed three times in ultrapure water and then dehydrated through a graded series of ethanol solutions (25%, 50%, 75%, 95%, 100%) by immersing them in each solution successively for 15 min. each. The 100% ethanol step was repeated twice and then the mats were critically point dried in a carbon dioxide bomb. The resulting "freeze-dried" specimens were mounted on SEM sample stubs using silver paint and coated with a thin layer (50 nm) of Au-Pd. The samples were viewed using a Hitachi SEM operating at 8 keV.

Transmission Electron Microscopy (TEM). For TEM, mat samples were prepared as described above for SEM except for the following changes: Two sets of TEM samples were prepared in parallel; those destined for ultrastructural examination only were treated with 2% (w/v) aqueous uranyl acetate for one hour after the osmic acid step. For the samples to be analysed by TEM-EDS, mat pieces were fixed by glutaraldehyde only and the Os and U were left out to avoid interference with naturally occurring metals and minerals in the samples. Both sets of TEM samples were treated similarly after the 100% ethanol step. They were immersed in a solution of 50:50 ethanol:acetone (15

min.) then 100% acetone (15 min), follwed by an overnight immersion in 50:50 acetone:Epon resin. The following morning the samples were embedded in 100% Epon resin in flat 21-well embedding moulds and allowed to cure for 48 hours at 60°C. Ultrathin (60-nm) sections were cut using a Reichert-Jung Ultracut E ultramicrotome equipped with a diamond knife. The sections were collected on 200-mesh copper grids and post-stained with 2% (w/v) uranyl acetate (aq) and 2% (w/v)Pb citrate (aq) if not destined for elemental anaysis.

For ultrastructural observations the sections were viewed using a Philips EM300 transmission electron microscope operating at 60 keV with a liquid nitrogen cold trap in place. Alternatively, sample for elemental analysis by energy-dispersive x-ray spectrosopy (EDS) were viewed using a Philips EM400T equipped with a model LZ-5 light element detector and an exL multichannel analyser (Link Analytical).

Environmental scanning electron microscopy (ESEM). Small (about 5mm diameter) pieces of living mat were removed from sample vials immediately prior to viewing in the ESEM using sterile forceps and placed on 25 mm diameter 0.22μm pore size polycarbonate filters. The filters served as a supporting substrate and were kept hydrated by placing them on wet Whatman No. 2 filter paper within closed glass Petri dishes. In this way the samples were transported to the microscope. For viewing, small pieces of the filters, holding the mat material, were cut out and placed on 1-cm diameter cylindrical metal slugs using double-sided carbon tape. These were placed within a metal cup in the Peltier stage and provided thermal coupling to the stage temperature controller.

All images were collected using a Philips XL30 ESEM equipped with a field emission electron gun. Within the ESEM, mat samples were kept at a temperature of 3°C using a Peltier cooling stage.

The water vapour pressure was set at 5.4 Torr, giving a relative humidity in the sample chamber of 95%. This level was chosen through trials which showed that it allowed full hydration of the specimen but with only a thin film of water present to allow details to be seen. Accelerating voltage was set at 20 keV and images were collected digitally using the ESEM software.

ESEM-EDS. The ESEM was equipped with a Princeton-GammaTech energy dispersive x-ray spectrometer optimised for light element detection. The instrumentation allowed bulk elemental composition to be determined as well as relative atomic proportions within the sample. In addition, the EDS system can interface to the imaging capabilities of the ESEM, allowing the production of elemental maps.

X-ray collection was performed using an accelerating voltage of 20 keV for 100s live time. This generally allowed a total count of 100 000 to be achieved with good spectral resolution. Under these conditions beam penetration into the sample was at most 1-2 μm based on a Monte Carlo simulation with Si as the matrix material. "Standardless" quantitative analysis allowed estimates of relative proportions of elements to be made within an error margin of 0.1%.

RESULTS AND DISCUSSION

Site Description. The Ancaster sulfur spring is located within the Niagara escarpment region of southwestern Ontario, Canada. The dominant bedrock type is dolomite with interbedded shales and gypsum as the other major rock-forming strata. The spring was originally a well for a local farm and, as such, was enclosed in a vertical galvanised steel pipe approximately 1 m in diameter. A round

plastic cover was originally installed to cap the spring but at present lies within the galvanised pipe in a near vertical position, almost completely submerged. At its source, the spring is at least 1.5 m deep (no bottom could be felt on probing to this depth). Water, emitting a strong smell of sulfide, flows out of the source at the head of a small roadside ravine and flows, perpendicular to the road, down the ravine, forming a small channel from 2 to 5 m wide and an average water depth of 5 to 10 cm. The ravine sides are steep and are abundantly vegetated with grasses, small herbaceous plants and shrubs. Large trees, typical of the local mixed hardwood forests, overhang the spring and its channel so that the major portion of sunlight recieved occurs during the cold months of the year. The spring source and channel are consequently the depositiory for large numbers of leaves and twigs, which form substrata for the growth of abundant microbial mats in the spring and its channel; the bed of the channel consists of mixed regions of gravel and clay.

Water Chemistry. The water flows from the source year round with a relatively constant temperature of 9°C and a pH of 7.1. An estimate of the redox potential using a hydrogen electrode gave a value of -335 mV only 8 cm below the water surface; the types of microorganisms found to dominate the spring's mat community (described subsequently) substantiated the observation that the spring waters were anoxic. We analysed three types of water samples from the spring: source water, downstream water, and mat pore water. The levels of dissolved ionic species measured were nearly identical for the spring waters (source and downstream) but there were some important differences noted in comparing the spring waters to mat pore waters. Most of the elements which were present in measurable quantities were present at slightly higher (1.5-2 times) levels in the mat pore water than in the general spring water with a few notable exceptions where certain elements were substantially

more concentrated in the mat pore waters. Table One shows these levels and also gives a concentration factor for pore water versus spring water. Both C and P were present at levels 9.3 times higher in the pore water as compared to the spring water. Zn was 22 times higher while Mn, Ba, Mg, and Cd were slightly elevated in the pore water by approximately a factor of 2. Fe, while not detectable in the spring waters, was present at a level of 2.9×10^{-3} mM. Although Sr was not involved in geomicrobiological interactions (i.e., no Sr-containing minerals were found), it was interesting to note that Sr levels were fairly high (0.2 mM), as were Ca (4.3 mM), and Mg (2.0 mM) in all the spring water samples. These were reflections of the dominant bedrock type in the area, which is dolomite ($CaMg[CO_3]_2$) with interbedded gypsum ($CaSO_4 \cdot 2H_2O$) and celestite ($SrSO_4$). The source water for the spring likely runs through gypsum and celestite beds from which the sulfate and cations are dissolved with the sulfate being reduced to sulfide by bacterial activity to arise as H_2S in the spring at a concentration of approximately 3.8 mM.

General mat and spring characteristics:

Throughout the spring waters, both at their source and within the channel, a fluorishing microbial community existed in the form of microbial mats which covered all available submerged surfaces from stones to sticks, leaves and the walls of the culvert lining the spring source. However, many different types of mats, based on colour and, to a certain extent, on texture and growth habit were present in specific zones as determined by the physical and chemical characterisitcs of the spring itself. A gross segregation of mat types existed between mats present in the source well (high sulfide/high dissoved Fe and Zn/low or no oxygen) and those growing in the channel, after the spring water had emerged from the source by spilling over the lip of the well, which was almost level with

the ground. The channel or "downstream" mats appeared as white filamentous growth on all available substrates. Underneath the white layer, there was often a blue-green one and, if the mats were growing on the channel sediment, a black layer underneath the blue-green one. This simple layered structure was in contrast to the situation in the source well. Here, the mats were of various colours based upon predominance of particular phototrophic organisms; blue-green in areas with highest light exposure, pink, often under leaves or under the blue-green layer, and brown-green mainly below a depth of 20 cm in the source. The mats lining the walls of the well were a dark olive green to black colour. The arrangement of these mat types in relation to each other was complicated by the layering of leaves and other debris within the well itself and by the regions of strong water flow which formed two main vertical paths through the well to the exposed water surface.

Rationale for our Approach. Using a wide range of different microscopical techniques to look at the same sample can provide a detailed characterisation and insight that would not be possible using only one technique. Our observations give an overview of a very complex dynamic microbial community and show how several microscopical techniques, when used together, can give a comprehensive view of the characteristics of a sample from the perspective of a range of scales and chemical information. Light microscopy gives an overall view of the organisation of the mats and, since colours can be seen, gives some idea of the nature of the material being viewed. For example, different types of phototrophic bacteria can be recognised by their characteristic pigmentation and inorganic deposits such as colloidal sulfur and clay minerals can be differentiated from the cells.

Using the light microscopical observations as a sort of map, the samples can be dissected and looked at using a medium resolution scale instrument; SEM or ESEM. Both of these techniques

allow the topography and overall arrangement of cells in the mats to be seen on a micrometre to nanometre scale. Figures 1 and 2 show the comparative appearance of the same mat sample by conventional SEM (cryo-preservation [Fig. 1A] and chemical fixation/critical point drying [Fig. 1B and 2B]). In the conventional SEM preparations the native organisation of the mat has been lost through drying, collapsing, and loss of small particulate material. However, the shapes of large filamentous organisms could be clearly seen and their intertangled nature, forming the main mat fabric, appreciated. Elemental composition data could be obtained but its quality is compromised due to the need for coating of the specimen.

ESEM (Fig.2A) operates on the same scale of resolution as SEM but there is an important difference with regard to sample preparation. Since no preparation of mat material (other than cutting to an appropriate size) was required for ESEM, mats in their natural, unaltered state could be observed. The fully hydrated gel matrix surrounding the cells, their natural spatial orientation with respect to each other and chemically unaltered mineral and inorganic deposits (such as colloidal sulfur) could be observed "in situ". This allowed many important insights to be gained into aspects such as mat fabric organisation, distribution of microbial types, and their contribution to the inorganic chemistry of their surroundings. Upon seeing the extent and all encompassing nature of the gel matrix, it was easy to understand how this could be the site of steep chemical gradients between the cell and its environment.

On an even higher resolution scale, TEM complements the observations made by ESEM by revealing cellular ultrastructure and the nature of epicellular minerals. By relating the TEM and ESEM observations to those made by light microscopy and of the mats as they appeared in the field it is possible to ascribe particular fine structural details to specific microbial groups and elucidate their

place in the community as well as some of their possible activities. The Ancaster sulfur spring hosts a highly integrated group of diverse microorganisms and it is only through the use of multiple techniques that a sufficienat array of features can be observed in order to put together a coherent picture of this living, dynamic community and place it in the context of its natural environment.

Descriptions of the mat microorganisms. Light microscopy showed that there was a strong predictable correlation between mat colour and microbial community composition as based on morphologically conspicuous groups of bacteria. The main broad groupings upon which our observations were based were the cyanobacteria, purple sulfur bacteria, green sulfur bacteria, and the colourless sulfur oxidising bacteria. Due to the difficulty of disrupting mats and getting homogeneous samples, no successful attempts could be made to enumerate cells. The estimates given are qualitative observations of abundance in relation to the other cell forms present. As a result, it is acknowledged that the morphotypes described for each group of organisms represents the dominant form and these descriptions are meant to convey the overall "flavour" of the community.

Cyanobacteria. The dominant type of cyanobacterium present in the Ancaster sulfur spring was a filamentous, rapidly gliding type that was made up of cylindrical cells which occured in pairs along the filament (Figure 3). Each pair was separated from its neighbour by a much deeper septal constriction than that which existed between the cells in the pair itself. The ends of the filaments exhibited rounded poles and at no time over the course of many observations of samples taken during several different seasons, did these organisms show the presence of any differentiated cells such as heterocysts, akinetes, or hormogonia. Otherwise, they resembled members of the genus *Anabaena.*

The rapidly gliding filaments were often arranged in parallel lines and sometimes had accumulations of spherical colloidal sulfur deposits adhered to their surface. This observation was confirmed by using ESEM, which gave a positive identification of these structures as colloidal S deposits and also showed that the filaments existed within an extensive matrix of gel-like extracellular polymeric material (Figure3A). Within the cells were highly refractile inclusions which were lined up along the septum and occured in every cell comprising the filament (Figure 3B). These did not have the shape generally associated with gas vacuoles nor did the benthic growth habit of the cyanobacteria support the idea that gas vacuoles were present. Observations by ESEM and probing simultaneously by EDS showed that these structures had a very high S content as compared to the neighbouring cytoplasm in the same cell (Figure 4). By TEM, the cyanobacteria showed a radiating pattern of thylakoid membranes which delimited the chromatoplasm region (Figure 5). In the centre of the cell, densely packed small dark inclusions, the ribosomes, were situated. The cells often showed large (200 -500 nm diameter) electron dense inclusions (likely cyanophycin, a nitrogen storage compound) and numerous smaller (50-100 nm) electron transparent spherical bodies.

Despite extensive observations made of the mats by both epifluorescence and confocal scanning laser microscopy (Figure 3C) no other types of cyanobacteria appeared to be present in the spring. It is likely that the conditions present were prohibitive for the growth of these organisms so that only this type, apparently with the ability to withstand and even make use of the high H_2S levels present, was able to fluorish.

Purple sulfur bacteria. Three main morphological types of purple sulfur bacteria were seen in the Ancaster sulfur spring mats. The least often encountered were large (approximately 3 μm diameter)

oval, motile cells closely resembling members of the genus *Chromatium*. These possessed numerous spherical internal sulfur granules and had a faint pink colour (as seen by light microscopy) to help confirm their identity as purple sulfur bacteria. Also motile, and present in fairly large numbers (i.e., many were seen in every field of view) were small (approximately 700 nm diameter) cells which were pink when present in groups and each possessed 2 spherical sulfur granules; one at each pole of the cell. These were most numerous at mat edges and could be seen "burrowing" into the bulk of the mat.

The main type of purple sulfur bacteria responsible for forming the pink mats was a very small (ca 500 nm diameter) coccoid type which grew as very cohesive masses of cells enclosed in a gel-like polymeric matrix. TEM observations showed that each cell was curved around a sort of vacuole which is membrane-bound and oriented to be nearest the inner side of the curve (Figure 6). The much thinner region of cytoplasm between the vacuole membrane and the cell membrane on the inside of the curve was much less densely stained by the heavy metals used to provide contrast and this seemed due to the fact that this region was devoid of photosynthetic membrane structures. These were of the vesicular type common in many freshwater purple sulfur bacteria. Most of the cells also contained numerous spherical inclusions of various sizes which were located toward the outside of the curve and appeared less electron dense than the large singular crescent shaped vacuole. These were interpreted as holes left behind when their contents were lost during the embedding procedure or during interaction with the electron beam whereas the material in the large crescent shaped inclusion appeared to have been infiltrated with resin and preserved somehow. It seemed likely that the small spherical inclusions were either sulfur or carbon storage structures (e.g., poly-β-hydroxybutyrate). The former is more likely since PHB generally does not leave as clean a hole behind when it is removed during processing or beam interaction. Sulfur is easily lost and not amenable to observation

by transmission electron microscopy so that it is unfortunately impossible to ascertain its presence by analytical methods such as EDS. However the relatively new technique of environmental scanning electron microscopy (ESEM) allows viewing of hydrated specimens. Using this technique we were able to confirm (data not shown) that the small sperical inclusions in these cells were rich in sulfur and thus were likely intracellular accumulations of colloidal sulfur.

Green sulfur bacteria. Due to the typically small size of these cells, ascribing particular cell morphologies to this group relied on relating the light microscopy samples to mat colour and to parallel observations made of the same sample by ESEM and by TEM. The olive-green/brown mats which predominated below 20 cm in the source had masses of cells of a particular shape–long sinuous rods about 800 nm in diameter. By light microscopy (Figure 7A), masses of these cells, which often seemed to exclude any others in the field of view, had the same colour as the mats themselves. By confocal scanning laser microscopy these cells could be selectively viewed owing to their autofluorescent photosynthetic pigments (Figure 5B). ESEM observations of these cells showed mass accumulations of colloidal sulfur particles which often were visible by naked eye as white patches intermingled in the mat. The lack of P,C,N signatures by ESEM-EDS and the wide size range (20nm to 1.2 μm) of these spherical particles confirmed that these were colloidal sulfur and not small unicellular S-rich bacteria (Douglas and Douglas, in review).

TEM observations of these mats showed that there were at least two types of green sulfur bacteria, based on ultrastructure, present in the Ancaster sulfur spring (Figure 8). All showed a Gram-negative bacterial wall structure and were 0.8-1.0 μm in diameter with each showing the numerous peripheral chlorosomes diagnostic for green sulfur bacteria. The cells resembled those typical of

Chlorobium by their rod-shaped morphology and non-motile nature, often occuring in chains.

The first ultrastructural type was surrounded by multiple layers of a proteinaceous paracrystalline surface layer (an S-layer), revealed by tangential sections to have a hexagonal symmetry pattern (Figure 8A and C). This was generally overlain by a loose capsule and appeared to be formed more of discontinuous plates than as a continuous uniform surface layer as is more typical for these structures. A variation was seen on *Chlorobium*-like cells which also had an S-layer but this was a single layer, and had a very different form. In cross-section, the structural subunits of theis S-layer appeared to be Y-shaped, with the stem of the Y meeting the cell's outer membrane (Figure 8D).

The second main structural variant of these *Chlorobium*-like cells was one which had no continuous extra surface layers beyond its gram-negative envelope, but was covered in numerous spinae (Figure 8B and C). These proteinaceous appendages are not much discussed in the recent literature but are often seen in on bacteria in environmental samples. On the Ancaster sulfur spring green sulfur bacteria the spinae were of varying lengths and of average diameter 27 nm or 36 nm; two main size classes possibly representing different species of green sulfur bacteria. The functions of spinae and S-layers are not well known but both types of structures are commonly observed on cels from *in situ* samples. However, in the Ancaster sulfur spring, the spinae of the green sulfur bacteria have a postulated role in elemental sulfur deposition, based on ESEM observations of samples in parallel with light microscopy and TEM (Douglas and Douglas, in review).

The brown-green mats were also abundantly populated by very thin (200 to 300 nm diameter) extremely long filaments which often protruded from the mats and had their ends hidden within them. These cells were featureless, appearing as long thin threads with no visible septa and could not be

positively correlated with organisms seen by ESEM or TEM (Figure 9). They superficially resemble either the green filamentous sulfur bacterium *Chloroflexus* or the filamentous *Methanosaeta concillii*, and given the prevailing environmental conditions, identification as either a methanogen or as a green sulfur bacterium is possible.

Colourless sulfur oxidising bacteria. These bacteria were not seen in the source mats but were the predominant microbial type in the downstream mats which lined the stream channel from the edge of the source pool to the point, 10-15 m downstream, where they diminished in abundance and disappeared altogether as available sulfide (and other reduced forms of sulfur) was depleted and oxygen levels were sufficiently high to inhibit growth of these bacteria. Examination of the mats by light microscopy and ESEM revealed at least two types of filamentous colourless sulfur oxidising bacteria and numerous small unicellular colourless sulfur oxidising bacteria (Figure 10). The latter were occluded within masses of colloidal sulfur particles but could be observed in abundance in laboratory bottle cultures. These were simple samples of mat plus spring water which were placed in bottles, filled to the top and tightly screw-capped. These were left to stand in the laboratory for several weeks until the white colour showed a significant decrease, indicating that all the available sulfide had been used up and the organisms were now using stored elemental sulfur to generate energy. Light microscopical observations of the samples at this transition stage showed very numerous apparently identical small bacteria with spherical colloidal sulfur particles closely associated with them (Figure 10B). These were commonly enclosed in veils of gel-like extracellular polymeric material and, in this form, may have been the major organisms responsible for forming the delicate white hair-like filaments which were macroscopically visible in the stream channel. Intuitively, the

filamentous forms of colourless sulfur oxidising bacteria would be more likely candidates for forming these structures but, even in fresh samples from the site they were far less numerous than the veiled unicellular bacteria.

Minerals in the Mats. *General trends.* The only mats which showed extensive mineral formation (except for colloidal sulfur) were the black-green mats which lined the culvert walls at the source. These comprised mainly unicellular bacteria which (by TEM) proved to have abundant mineral precipitates closely associated with them, often completely encrusting the whole cell. The mineralisation became more extensive with depth in the biofilm (i.e., with proximity to the culvert wall). By light microscopy, cells from this region were mainly unicellular bacteria of numerous shapes and sizes, speaking of a complex interplay of diverse physiologies. However, the mats which grew on the culvert wall showed a particular layering of microbial types (Figure 11). Closest to the wall were numerous small unicellular bacteria of varying morphologies and these generally were encrusted with fine-grained granular to fibrous mineral precipitates which were shown to be by TEM-EDS to be Fe and Zn sulfides (data not shown). This part of the mat was also rich in cell wall debris, membrane fragments, and empty sheaths. Notably, cells completely encrusted with minerals were often adjacent to completely unmineralised cells of a different morphology and size, indicating a likely effect of particular metabolic activities on local microenvironmental geochemistry which, in turn, determined the precipitation of specific mineral types. Overlying the layer of mineralised small bacteria was a zone of uniformly unmineralised bacterial cells and their associated debris. Topmost (farthest from the culvert wall) was a layer of cyanobacteria and closely associated (often within the same sheath) filamentous bacteria of another type. It is possible that they prefer to cluster around the

outlined the cell as seen in cross section and were presumptively identified as metal sulfide precipitates. The Cl ions were likely adsorbed onto the sulfide minerals or possibly held within their matrix. The precipitates were too small to permit electron diffraction patterns to be generated but in general nascent minerals on cell surfaces are highly hydrated and therefore do not give clear patterns representative of a definite crystallographic structure that would allow mineral identification.

The platy minerals seen, especially those which were not closely associated with cells, were likely pre-existing mineral precipitates that adsorbed to the polymer matrix produced by the cells. these contained Si and often were able to produce some spots with electron diffraction, but were still too small to give an extensive enough array of spots to allow for mineral identification. It was likely, given the presence of surrounding soils and the local pedology, that these were clay minerals, most likely washed into the spring by rainfall.

We are presently planning to continue our studies of the Ancaster sulfur spring by conducting phylogenetic analysis of the microbial community and acquiring more detailed geochemical information including biogenic gases to help us elucidate the relationship between the microorganisms and their environment.

ACKNOWLEDGEMENTS

Transmission electron microscopy and conventional scanning electron microscopy was performed at at the University of Guelph. The TEM is part of the NSERC Regional STEM facility directed by Dr. Terry Beveridge and is supported by funds from the Natural Sciences and Engineering Research Council of Canada. Environmental scanning electron microscopy and all light microscopy (including CSLM) was performed at JPL. The financial support of NASA's Origins program and of JPL is

cyanobacteria in order to benefit from the metabolites they may release.

The minerals seen in our samples fell into two main structural categories (Figure 12). Small fine-grained minerals tended to be present on cell surface layers; these tended to be sulfide minerals, either Zn or Fe dominated. Fractured minerals which appeared to be cross-sectioned plates were usually external to groups of cells but trapped within their EPS matrix. By TEM-EDS these were silicates which all contained Fe and, when well removed from the vicinity of bacterial cells, also had small amounts of Al, K, and Mg incorporated. Platy precipitates that were small and localised on cell surfaces were Fe rich with no other element detectable except Cl. Figure 23 shows a remarkable example of ZnS deposition. These "Zn tubes" seen by ESEM appear hollow and may be the remaining sheaths of organisms that promoted the formation of ZnS on their surfaces.

We interpret our results as follows: Bacterial cell surface layers (walls, capsules, S-layers, sheaths, etc.) are potent metal ion binding agents which can scavenge metal ions from solution, effectively concentrating them (Beveridge and Fyfe 1984; Beveridge 1986). In the Ancaster sulfur spring, the conditions of neutral pH and low Eh are such that Fe and Zn can remain soluble (Stumm and Morgan, 1996). The majority of these ions likely derive from the metal culvert which encloses the spring at its source and represent those which have not been immobilised into solid phases by adsorption to cells or pre-existing minerals such as clays. The dark pigmentation of the mats and the lack of any orange deposits, together with our chemical data indicate that the Fe was predominantly present in its reduced form (Fe^{2+}). The small fine grained sulfide mineral precipitates which formed on the cell surfaces likely began as Fe and/or Zn bound to the cell surface. This effective concentration of metals promoted the binding of counterions which in the Ancaster sulfur spring were predominantly S^{2-} or possibly Cl^-. Consequently, when these small mineral grains were seen, they

REFERENCES

D'Amelio ED, Cohen Y, Des Marais D (1989) Comparative functional ultrastructure of two hypersaline submerged cyanobacterial mats: Guerrero Negro, Baja California Sur, Mexico, and Solar Lake, Sinai, Egypt. In: Cohen Y, Rosenberg E (eds) Microbial Mats: Physiological Ecology of Benthic Microbial Communities. ASM Washington, D.C. pp 97-113

Belkin S, Jannasch HW (1989) Microbial mats at deep-sea hydrothermal vents; new observations. In: Cohen Y, Rosenberg E (eds) Microbial Mats: Physiological Ecology of Benthic Microbial Communities. ASM Washington, D.C. pp 16-21

Beveridge TJ, Fyfe WS (1984) Metal fixation by bacterial cell walls. Can J Earth Sci 22: 1893-1898

Beveridge TJ (1986) The immobilization of soluble metals by bacterial walls. Biotech Bioeng 16: 129-139

Canfield DE, Des Marais DJ (1993) Biogeochemical cycles of carbon, sulfur, and free oxygen in a microbial mat. Geochim Cosmochim Acta 57: 3971-3984

CohenY, Jørgensen, BB, Padan E, Shilo M (1975) Sulfide-dependent anoxygenic photosynthesis in the cyanobacterium *Oscillatoria limnetica*. Nature 257:489-492.

gratefully acknowledged. We would also like to thank Dr. Graeme Spiers of the Ontario Ministry of Natural Resources for ICP analysis.

Cohen Y, Jørgensen BB, Revsbech NP, Poplawski . (1986) Adaptation to hydrogen sulfide of oxygenic and anoxygenic photosynthesis among cyanobacteria. Appl Env Microbiol 51:398-407

Garlick S, Oren A, Padan, E (1977) Occurrence of facultative anoxygenic photosynthesis among filamentous and unicellular cyanobacteria. J Bacteriol 129:623-629

Jannasch HW (1995) Microbial interactions with hydrothermal fluids. Geophysical Monograph 91:273-296

Jørgensen BB (1982) Ecology of the bacteria of the sulfur cycle with special reference to anoxic-oxic interface environments. Phil Trans Roy Soc London B 298:543-561

Jørgensen BB, Gallardo, V (1999) *Thioploca* spp.: filamentous sulfur bacteria with nitrate vacuoles. FEMS Microbiol Ecol 28: 301-313

Larkin JM, Strohl WR (1983) *Beggiatoa, Thiothrix,* and *Thioploca*. Annu Rev Microbiol 37:341-367

Nelson DC (1989) Physiology and biochemistry of filamentous sulfur bacteria In: Schlegel HG (ed) Autotrophic Bacteria. Elsevier, Amsterdam pp. 219-237

Nelson DC, Jannasch HW (1983) Chemoautotrophic growth of a marine *Beggiatoa* in sulfide

gradient cultures. Arch Microbiol 136:262-269

Oren A, E Padan (1978) Induction of anaerobic photoautotrophic growth in the cyanobacterium *Oscillatoria limnetica*. J Bacteriol 133:558-563

Oren A, Padan,E Arron M (1977) Quantum yields for oxygenic and anoxygenic photosynthesis in the cyanobacterium *Oscillatoria limnetica*. Proc Natl.Acad Sci USA 74:2152-2156

Pfennig N, Trüper HG (1989) Anoxygenic Phototrophic Bacteria In: Staley JT, Bryant M.P, Pfennig N, Holt, JG (eds) Bergey's Manual of Systematic Bacteriology (Vol. 3) Williams and Wilkins, Baltimore. pp 1635-1653

Steudel R (1989) On the nature of "elemental sulfur" (S^0) produced by sulfur-oxidizing bacteria: a model for S^0 globules. In: Schlegel HG (ed) Autotrophic Bacteria. Elsevier, Amsterdam. pp 289-303

Stumm W Morgan JJ (1996) Aquatic Chemistry: Equilibria and Rates in Natural Waters, 3rd Edition. John Wiley and Sons, Inc. New York

FIGURE LEGENDS

Figure 1: Appearance of the mats by conventional SEM.. Image **A** shows source mat preserved by rapid freezing in liquid nitrogen ("cryo-prep"). Numerous filaments, presumably cyanobacteria, based on their size, are accompanied by small granular structures (mineral grains and/or unicellular bacteria and debris). The extracellular polymeric matrix is present as a tattered veil shrouding some of the cells (compare to Figure 1). In **B** a chemically prepared and Au/Pd-coated specimen is shown as viewed by conventional SEM. The chain of large cells in the top of the image is a cyanobacterium. Note the condensed material on the cyanobacterial cells and the lack of small unicellular bacteria. The shapes of the cells can be clearly seen.

Figure 2: A comparison of conventional SEM (**A**) and ESEM (**B**). The same mat specimen was viewed using each technique. Although the shapes of cells can often be more easily seen by conventional SEM, the actual spatial relationships among cells and the nature of the extracellular polymeric matrix in which they are embedded can only be seen by ESEM (the arrow points to a cyanobacterial filament). In addition, sample material is lost during preparation for conventional SEM, possibly preferentially (e.g., unicellular bacteria are lost but the interwoven filamentous bacteria are retained).

Figure 3: ESEM (**A** and **B**) and confocal scanning laser micrographs of the filamentous cyanobacterium from the Ancaster sulfur spring. In **A** the arrow points to a region of the image where several long filaments can be seen in parallel. The organisms are embedded in a gelatinous

matrix of extracellular polysaccharide (EPS), visible as a sort of shroud in this image of a fully hydrated specimen. The EPS is particularly well visible to the left of the row of filaments. **B:** ESEM image of a single cyanobacterial filament. The locations of septa between the cells can be clearly seen. The arrow points to light coloured intracellular inclusions which give a very high sulfur signal relative to the general cytoplasm (see Figure 4).

Figure 4: Energy dispersive xray spectrosopy (EDS) spectra collected using the ESEM. Both spectra were taken from points along a cyanobacterial cell. Spectrum **A** was collected from one of the intracellular periseptal inclusions indicated in Figure 3B. Spectrum **B** is a representative spectrum from the general cyanobacterial cytoplasm. It is readily apparent that there is a much stronger sulfur signal in the inclusions, indicating that these may be intracellular sulfur depositions, structures previously unknown in cyanobacteria.

Figure 5: Transmission electron (TEM) micrograph of a thin sectioned cyanobacterial cell of the same species shown in Figure 3. This tangential section shows the radiating thylakoid membranes, accompanied by numerous phycobilisomes (proteinaceous light-harvesting structures) which appear as small, regularly arranged granular inclusions in the thylakoid region. Two nascent septa can be seen at the centre of the cell.

Figure 6: Transmission electron micrographs of thin sectioned pink mat from the spring source. The purple sulfur bacteria shown in these images were the dominant morphotype present and have an unusual form which does not conform to any descriptions in the literature. **A** shows a group of

cells surrounded by extracellular polymers, which appear as fibrils filling the area between cells. Numerous round holes (S) within are sites of sulfur deposition from which the sulfur was extracted during specimen preparation. The lower image (**B**) shows the detailed cellular features. The cells have a layered outer wall and numerous different cellular inclusions. One prominent feature is a large crescent shaped "vacuole" of unknown nature.

Figure 7: Phase light (**A**) and confocal scanning laser (**B**) micrographs of green sulfur bacteria from the brown-green mats at the spring's source. The long rod to filamentous morphology of these organisms is evident in these images.

Figure 8: Transmission electron micrographs of thin sectioned brown-green source mat. The green sulfur bacteria (see also Figure 7) are of various ultrastructural types but all are recognisable by the presence of peripheral, electron translucent ovoid features; the chlorosomes. Spinae (SP) and S-layers (SL) are proteinaceous structural features of these cells which may be characteristic of different species or strains.

Figure 9: Phase light (**A**) and ESEM (**B**) images of the numerous thin filaments seen in the brown-green source mats. By both methods, they were remarkably featureless; no septa or other morphologically distinctive could be seen.

Figure 10: Filamentous and unicellular colourless sulfur oxidising bacteria. **A:** The highly refractile inclusions in the filamentousform (SB) are sulfur inclusions. A cyanobacterial filament

(CB) is also present in this image. **B**: Numerous unicellular colourless sulfur oxidising bacteria, joined by an extensive polymer matrix, form veils when present in large masses. These were the dominant organisms forming the macrosopically visible white wisps in the downstream portion of the spring. By ESEM (C) the filamentous colourless sulfur oxidising bacteria are mostly difficult to see except for their numerous colloidal sulfur inclusions.

Figure 11: When mats from the culvert wall at the spring source are thin sectioned and viewed by TEM, a characteristic layering is seen. The left side of the image shows the mat region that was closest to the centre of the spring. Here, filamentous colourless sulfur oxidising bacteria (S) and cyanobacteria (C) exist in close proximity as in the downstream mats (see Figure 10). Closer to the source wall, unicellular bacteria of diverse morphotypes dominate and these are surrounded by mineral precipitates.

Figure 12: This TEM micrograph shows a detailed view of some of the minerals found in association with the bacteria growing on the culvert walls at the spring's source. The arrow at the upper centre indicates an empty bacterial sheath studded with abundant fine-grained minerals. Unmineralised bacterial cells (b) and the remains of mineralised ones (ML) coexist within the mats, indicating an influential role of the bacteria in mineral deposition. The minerals indicated by ML are typical of the Fe and Zn sulfides (often mixed) while PL indicates a detrital clay mineral.

Figure 13: A mass occurrence of these unusual "Zn tubes" was found in the source wall mats. This view by ESEM shows what appear to be mineralised sheaths; EDS analysis (data not shown)

Table One: ICP-MS data[a] for bulk spring water and mat pore water

Element	Detection Limits (mM)	Spring Water (mM)	Mat Pore Water (mM)	Concentration Factor[b]
Ba	7.28×10^{-6}	3.2×10^{-4}	6.2×10^{-4}	2.0
C	2.33×10^{-4}	1.99	18.6	9.3
Ca	2.50×10^{-4}	3.9	4.3	1.1
Cd	1.78×10^{-5}	0	4.4×10^{-5}	2.2
Cu	2.05×10^{-4}	n.d.	8.18×10^{-4}	n/a
Fe	8.95×10^{-4}	n.d.	2.87×10^{-3}	n/a
K	2.05×10^{-3}	7.7×10^{-2}	0.1	1.3
Li	5.76×10^{-4}	5.0×10^{-3}	5.8×10^{-3}	1.2
Mg	4.1×10^{-5}	1.1	2.0	2.0
Mn	1.8×10^{-5}	4.7×10^{-4}	9.7×10^{-4}	2.0
Na	8.70×10^{-4}	2.0	2.4	1.2
P	2.6×10^{-5}	5.4×10^{-4}	5.0×10^{-3}	9.3
S	3.12×10^{-4}	3.5	3.8	1.1
Si	3.6×10^{-4}	0.2	0.3	1.5
Sr	1.94×10^{-6}	0.2	0.2	0
Zn	5.82×10^{-4}	7.3×10^{-4}	1.6×10^{-2}	22.0

[a]The following elements were also measured but found to be below detection limits: Al, As, Be, Co, Cr, Mo, Ni, Pb, Rb, Sb, Se, Sn, Ti, U, V.

[b]The concentration factor represents the level to which elements in the pore water are higher than those in the bulk spring water.

indicated that the elements present were Zn and S in a 1:1 ratio.

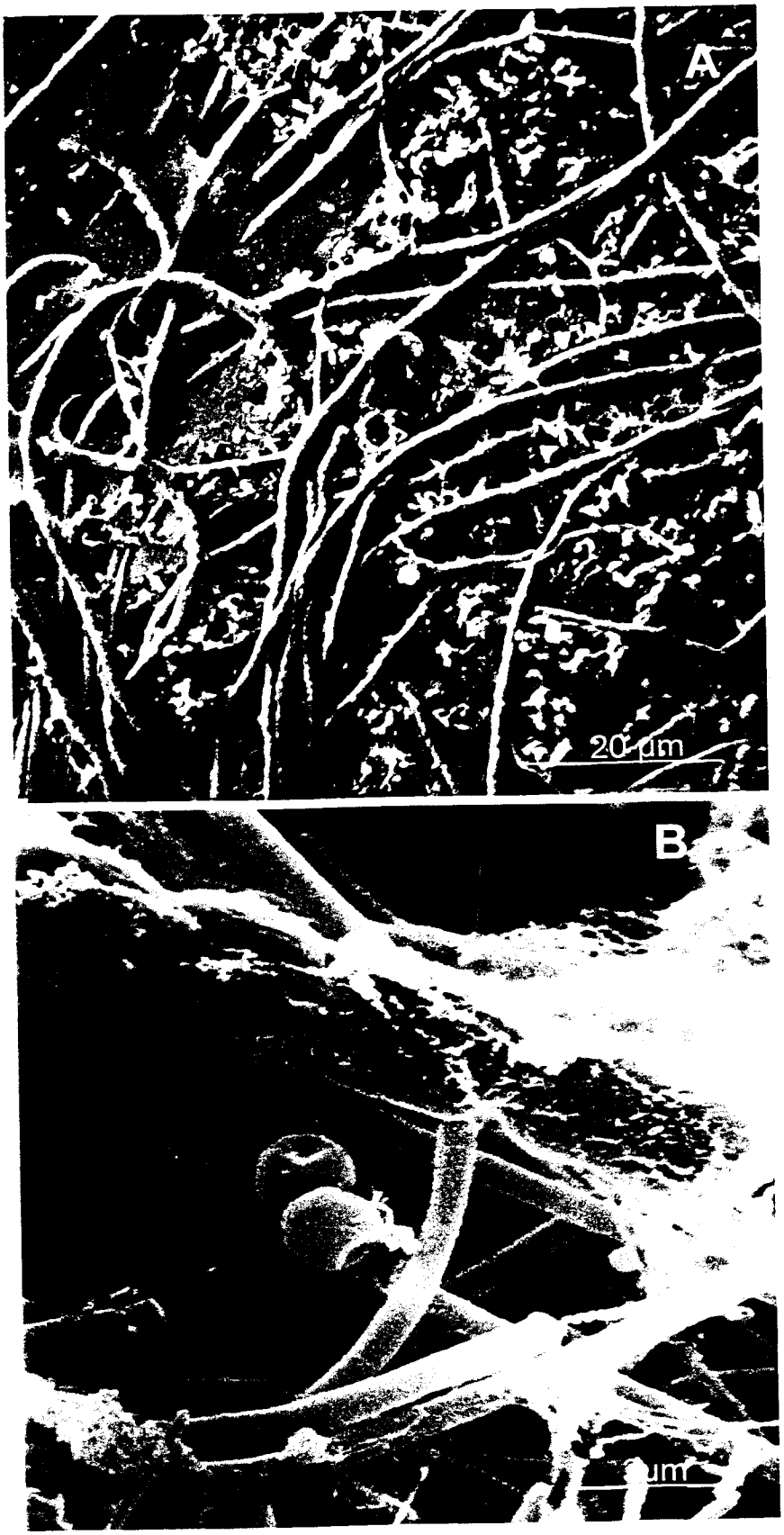
A
20 µm
B
µm

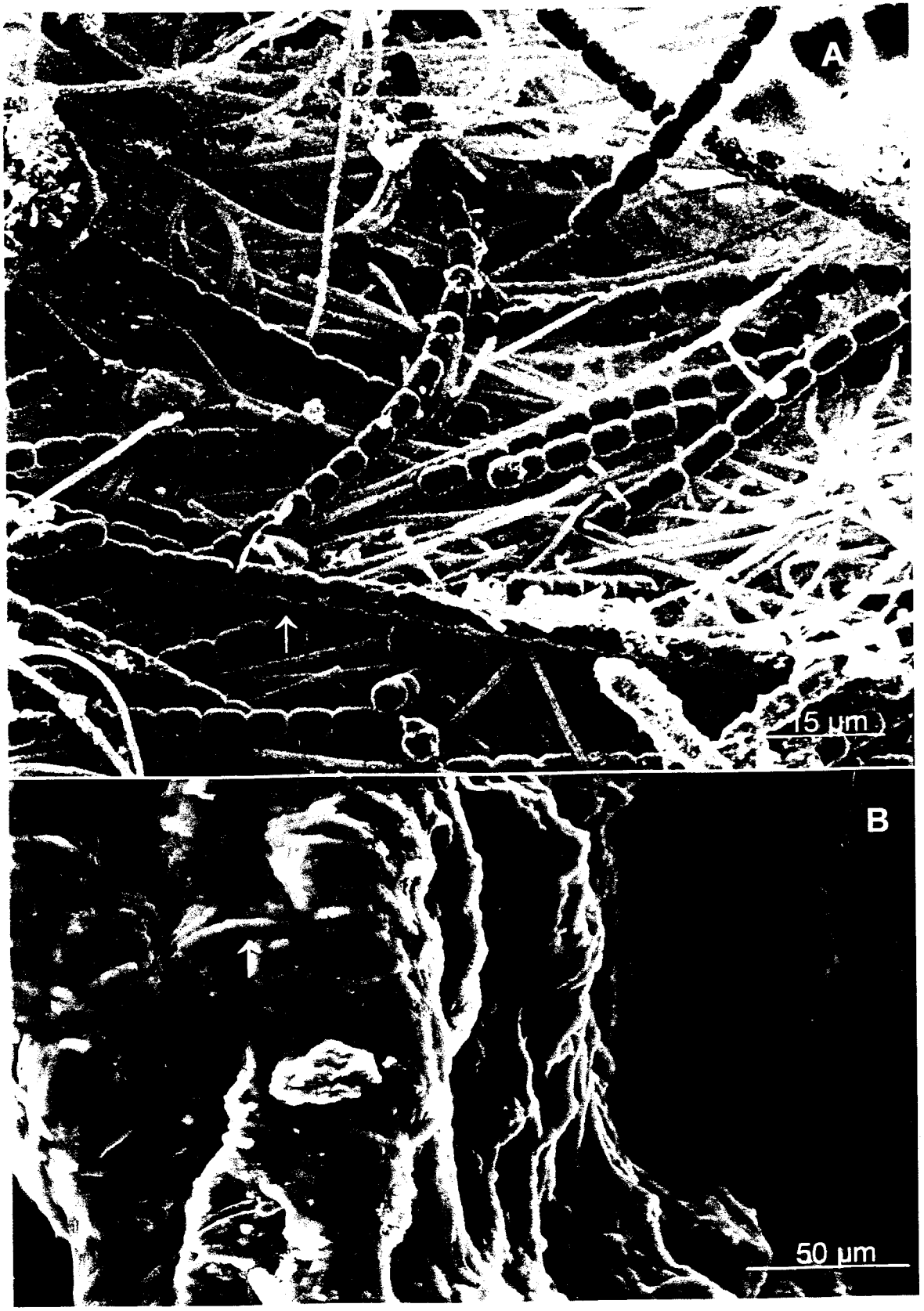
A
15 µm
B
50 µm

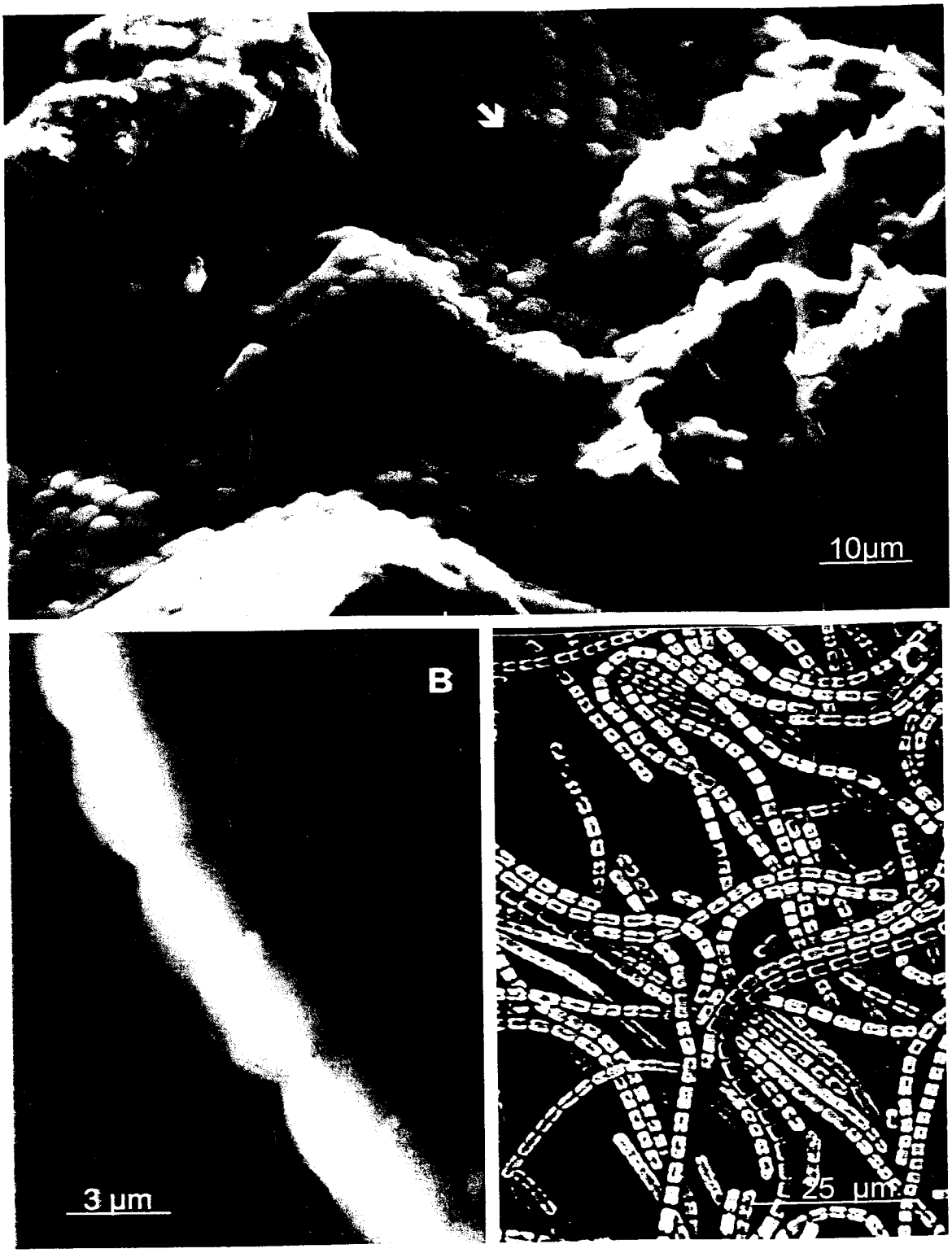
10µm
B
3 µm
C
25 µm

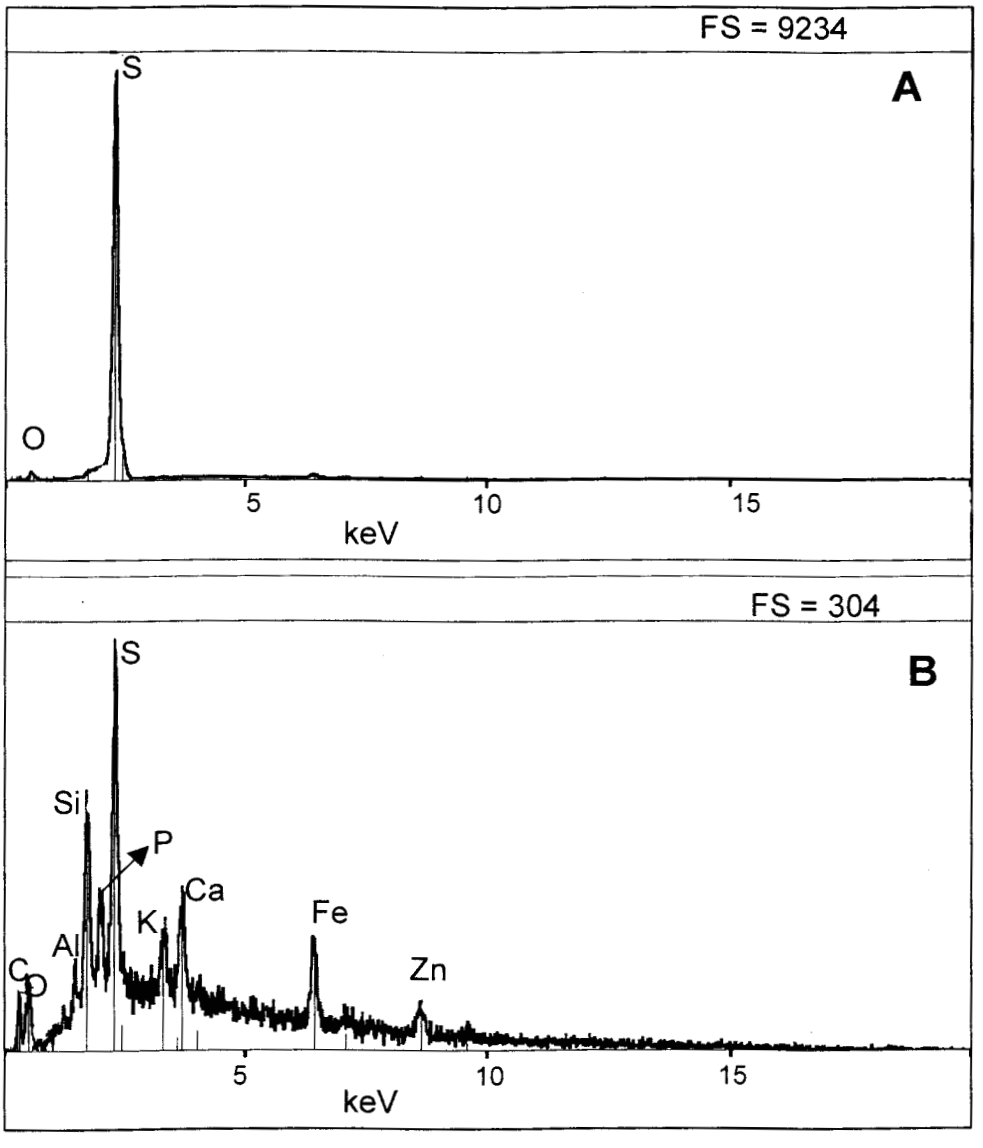
FS = 9234
A
S
O
5
10
15
keV
FS = 304
B
S
Si
P
Ca
K
Fe
Al
C
O
Zn
5
10
15
keV


S
B

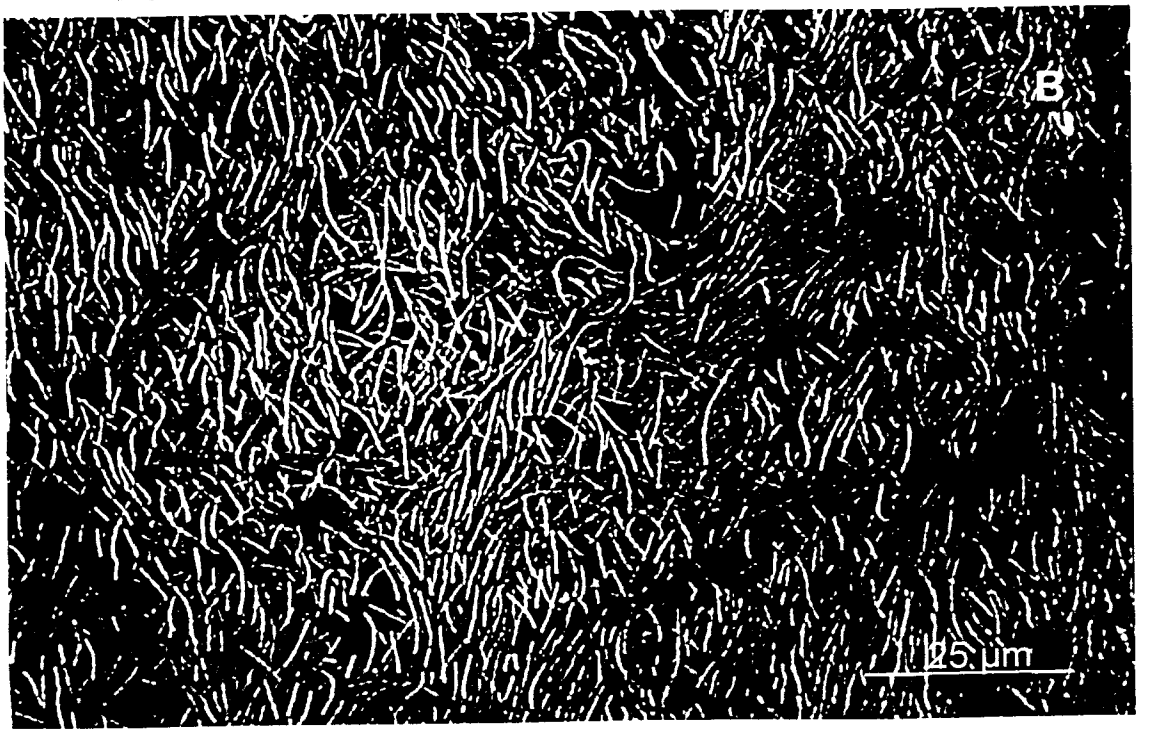
B
25 µm

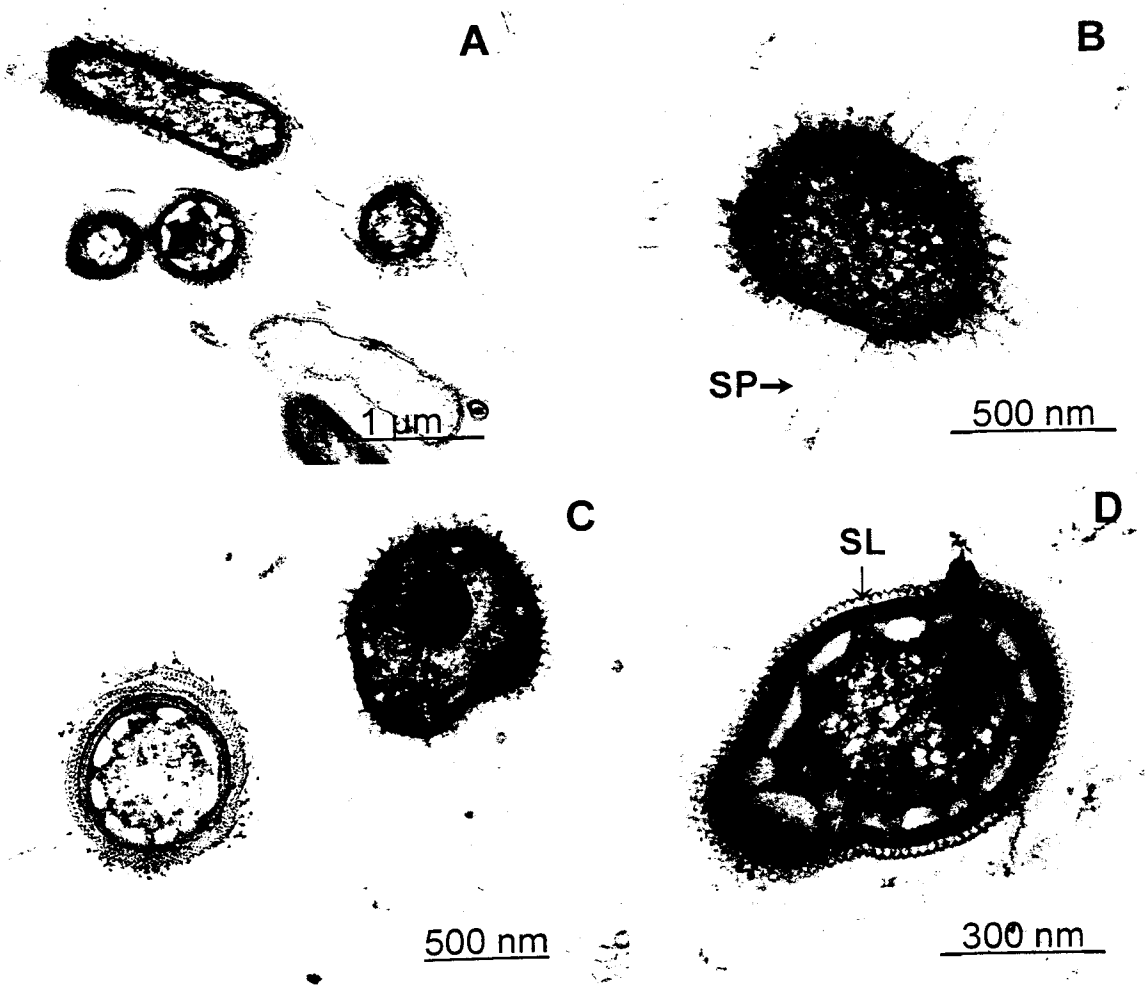
A
1 µm
B
SP→
500 nm
C
500 nm
D
SL
300 nm

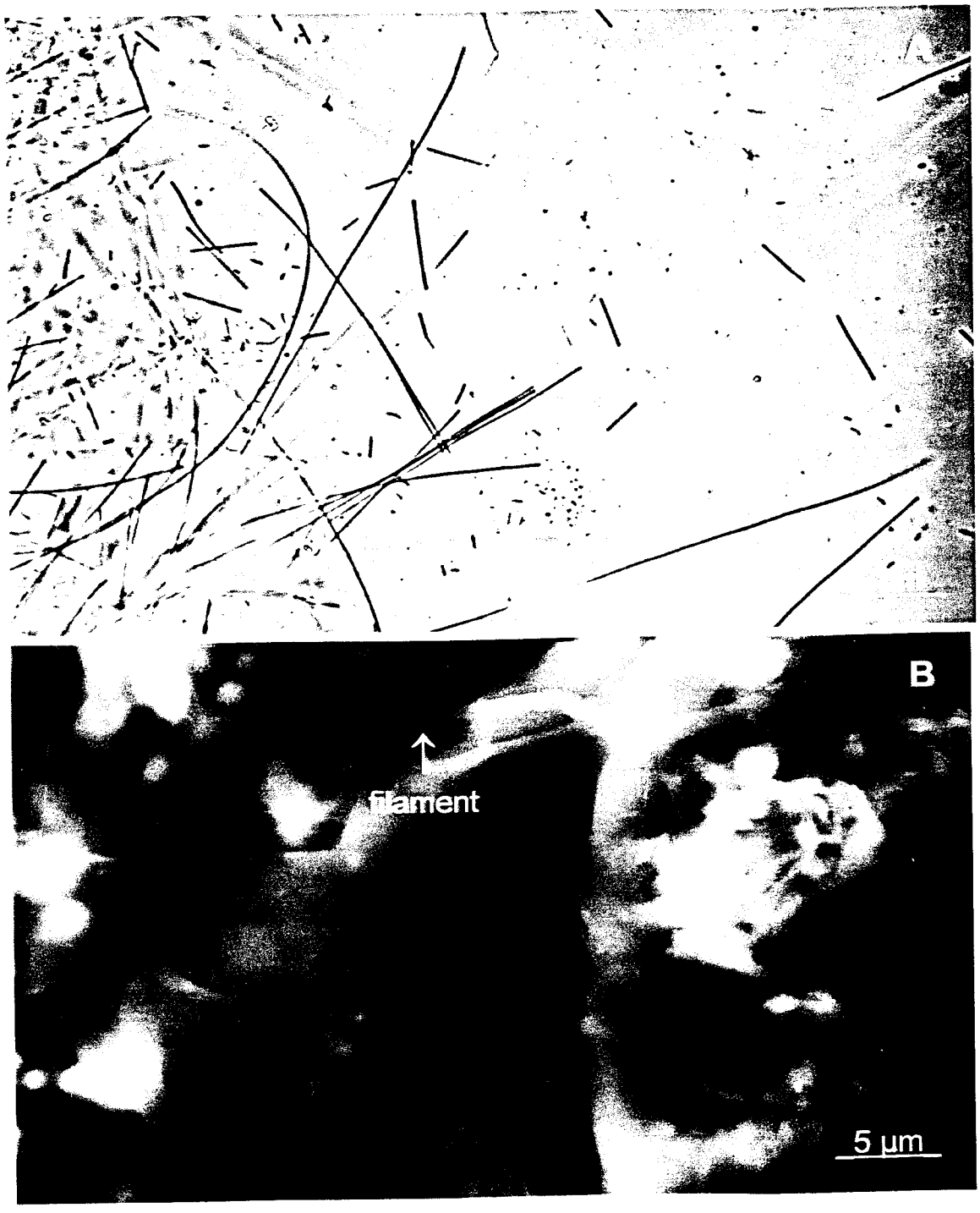
A
B
filament
5 µm

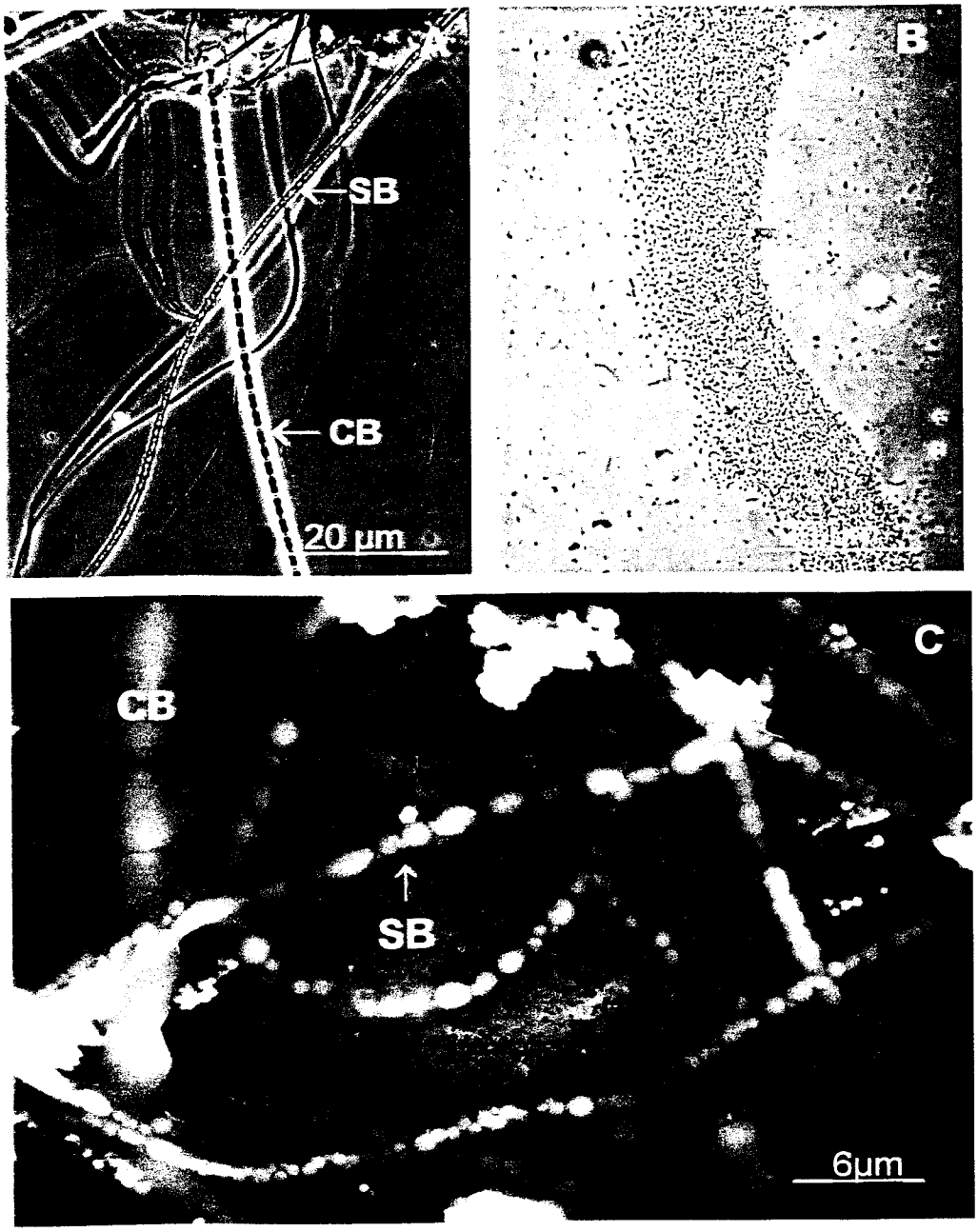
A
SB
CB
20 µm
B
C
CB
SB
6µm

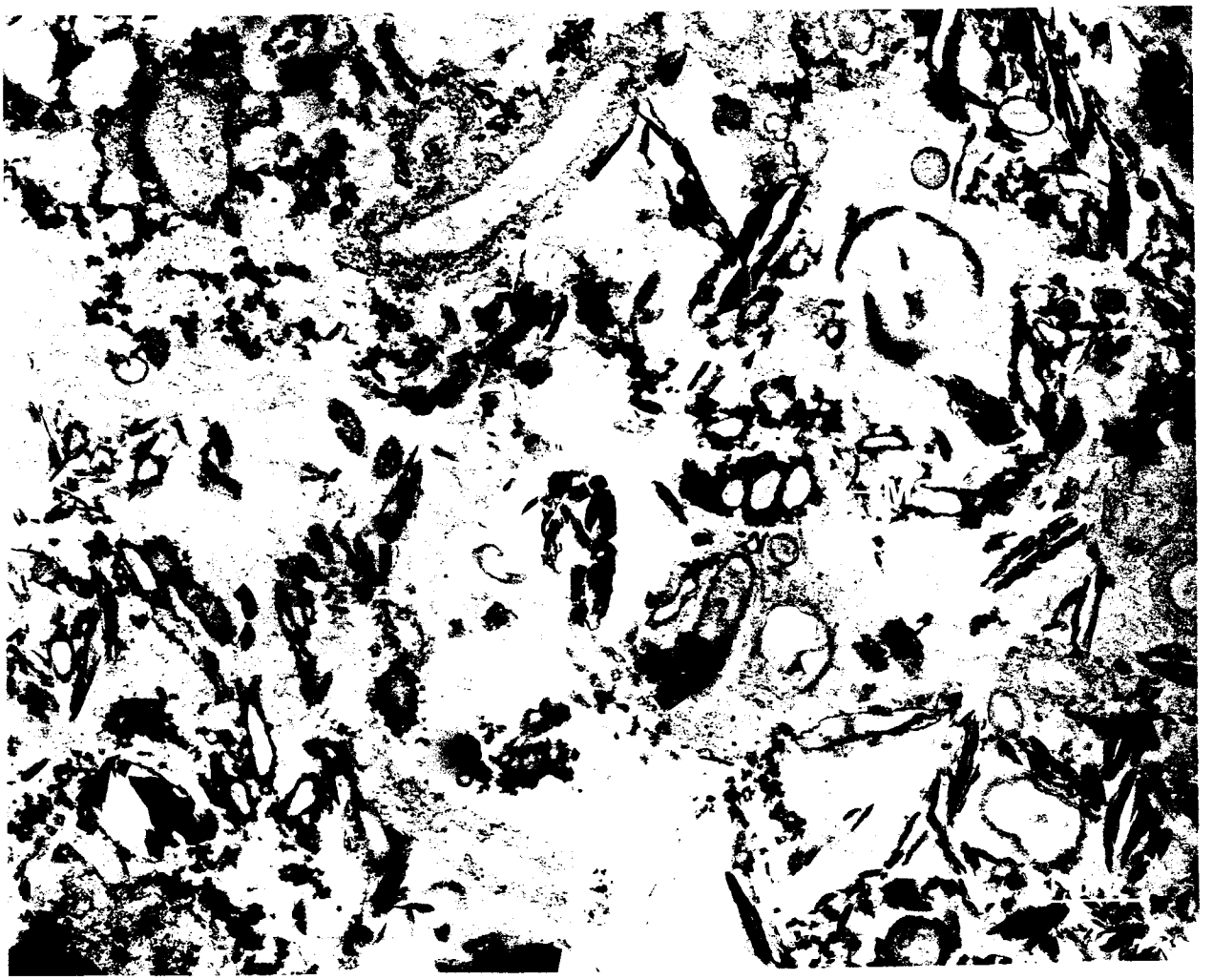


20 µm